Published OnlineFirst April 10, 2013; DOI: 10.1158/0008-5472.CAN-12-3839

Therapeutics, Targets, and Chemical Biology

Cancer Research

DOG1 Regulates Growth and IGFBP5 in Gastrointestinal Stromal Tumors

Susanne Simon[1,2], Florian Grabellus[1,3], Loretta Ferrera[6], Luis Galietta[6], Benjamin Schwindenhammer[1,3], Thomas Mühlenberg[1,2], Georg Taeger[1,4], Grant Eilers[7], Juergen Treckmann[1,5], Frank Breitenbuecher[1,2], Martin Schuler[1,2], Takahiro Taguchi[8], Jonathan A. Fletcher[7], and Sebastian Bauer[1,2]

Abstract

Gastrointestinal stromal tumors (GIST) are characterized by activating mutations of KIT or platelet-derived growth factor receptor α(PDGFRA), which can be therapeutically targeted by tyrosine kinase inhibitors (TKI) such as imatinib. Despite long-lasting responses, most patients eventually progress after TKI therapy. The calcium-dependent chloride channel DOG1 (ANO1/TMEM16A), which is strongly and specifically expressed in GIST, is used as a diagnostic marker to differentiate GIST from other sarcomas. Here, we report that loss of DOG1 expression occurs together with loss of KIT expression in a subset of GIST resistant to KIT inhibitors, and we illustrate the functional role of DOG1 in tumor growth, KIT expression, and imatinib response. Although DOG1 is a crucial regulator of chloride balance in GIST cells, we found that RNAi-mediated silencing or pharmacologic inhibition of DOG1 did not alter cell growth or KIT signaling *in vitro*. In contrast, DOG1 silencing delayed the growth of GIST xenografts *in vivo*. Expression profiling of explanted tumors after DOG1 blockade revealed a strong upregulation in the expression of insulin-like growth factor-binding protein 5 (IGFBP5), a potent antiangiogenic factor implicated in tumor suppression. Similar results were obtained after selection of imatinib-resistant DOG1- and KIT-negative cells derived from parental DOG1 and KIT-positive GIST cells, where a 5,000-fold increase in IGFBP5 mRNA transcripts were documented. In summary, our findings establish the oncogenic activity of DOG1 in GIST involving modulation of IGF/IGF receptor signaling in the tumor microenvironment through the antiangiogenic factor IGFBP5. *Cancer Res; 73(12); 3661–70. ©2013 AACR.*

Introduction

Gastrointestinal stromal tumors (GIST) are the most common mesenchymal tumors of the gastrointestinal tract and are characterized by activating mutations in the *KIT* or platelet-derived growth factor receptor α (*PDGFRA*) genes (1–3).

Imatinib mesylate (IM) is a small molecule inhibitor of several oncogenic tyrosine kinases, including KIT and PDGFRA. About 85% of patients with metastatic GIST derive substantial clinical benefit from IM treatment; however, imatinib does not cure metastatic GIST and the majority of patients eventually progress. Second, imatinib-resistant KIT mutations within the ATP-binding and activation loop domain are commonly found in IM-resistant GIST and are believed to be the major mechanism of resistance (4–7).

The protein DOG1 (discovered on GIST-1) encoded by *ANO1* (also known as *TMEM16A)* is a calcium-dependent chloride channel (CaCC; refs. 8–10). CaCCs are involved in diverse physiologic processes including gastrointestinal rhythmic contractions (11, 12). Notably, DOG1 was found to be highly expressed both in GIST (13) and in interstitial cells of Cajal (ICC), the putative cell-of-origin of GIST (14, 15).

In clinical practice, DOG1 is a sensitive immunohistochemical marker for GIST and is preserved in 36% of GIST that lack KIT expression or activating mutations of *KIT* or *PDGFRA* (16–18). However, DOG1 biologic functions have not been characterized in GIST. To shed light on the relevance of DOG1 for GIST tumorigenesis, we evaluated the impact of DOG1 expression and activity in various GIST models, both *in vitro* and *in vivo*.

Materials and Methods

Cell lines

GIST-T1 and GIST882 were established from human, untreated, metastatic GISTs. GIST-T1 contains a 57bp deletion in *c-KIT* exon 11 (19). GIST882 harbors a homozygous exon 13 missense mutation, resulting in a single amino acid substitution, K642E (20). GIST48 and GIST430 were established from GIST that had progressed, after initial clinical response, during

Authors' Affiliations: [1]Sarcoma Center, Departments of [2]Medical Oncology, [3]Pathology and Neuropathology, [4]Trauma and Orthopedic Surgery, [5]Visceral and Transplant Surgery, West German Cancer Center, University Duisburg-Essen, University Hospital Essen, Germany; [6]Istituto Giannina Gaslini, Genova, Italy; [7]Department of Pathology, Brigham and Women's Hospital, Harvard Medical School, Boston, Massachusetts; and [8]Division of Human Health and Medical Science, Graduate School of Kuroshio Science, Kochi University, Nankoku, Kochi, Japan

Corresponding Author: Sebastian Bauer, Department of Medical Oncology, West German Cancer Center, University Hospital Essen, Hufeland str. 55, 45122 Essen, Germany. Phone: 49-201-723-8501; Fax: 49-201-723-5996; E-mail: sebastian.bauer@uk-essen.de

doi: 10.1158/0008-5472.CAN-12-3839

Published OnlineFirst April 10, 2013; DOI: 10.1158/0008-5472.CAN-12-3839

IM therapy. GIST48 has a primary, homozygous exon 11 missense mutation (V560D) and a heterozygous secondary exon 17 (kinase activation loop) mutation (D820A). GIST430 has a primary heterozygous exon 11 in-frame deletion and a heterozygous secondary exon 13 missense mutation. GIST882B, GIST48B, and GIST430B are sublines, which despite retaining the activating KIT mutation in all cells, express KIT transcript and protein at essentially undetectable levels. GIST62 was derived from an untreated KIT-positive GIST with KIT exon 11 in-frame mutation, but the cell line, despite retaining the activating KIT mutation in all cells, expresses KIT transcript and protein at essentially undetectable levels (21). GIST5 and GIST474 were established from imatinib-treated GISTs, and lacked KIT expression in the primary and subsequent cultures, although they retain the KIT exon 11 mutations of the parental GIST population.

Stable short hairpin RNA transfection

Short hairpin RNA (shRNA) lentivirus for human DOG1 (NM_018043) was obtained from Sigma-Aldrich (MISSION shRNA Lentiviral Transduction Particles TRCN0000040263). GIST cells were grown to 80% confluence and then infected with 1 multiplicity of infection of either nontargeting scrambled shRNA (SHC002V) control particles or DOG1 shRNA lentiviral particles in medium containing 8 μg/mL polybrene. Fresh medium containing 4 μg/mL puromycin was added after 48 hours to select for puromycin-resistant cells.

Reagents and antibodies

Imatinib mesylate (IM) was purchased from Selleck Chemicals. 17-N-Allylamino-17-demethoxygeldanamycin (17-AAG) was purchased from Calbiochem (Merck). A rabbit polyclonal antibody against KIT was from DAKO and a monoclonal rabbit antibody against DOG1 was from Diagnostic BioSystems. Polyclonal rabbit antibodies for phospho-KIT Y703 were from Cell Signaling. β-actin antibody was purchased from Sigma-Aldrich.

In vitro assays

BrdUrd incorporation assay. Cells were incubated with 1 mmol/L bromodeoxyuridine (BrdUrd) for 2.5 hours (GIST-T1) or 24 hours (GIST882) at 37°C and processed using the fluorescein isothiocyanate (FITC) BrdUrd Flow Kit (BD Biosciences) following the manufacturer's instructions. Briefly, 1.5×10^6 trypsinized cells were fixed, permeabilized, and digested with DNAse. Cells were then stained with FITC-conjugated anti-BrdUrd and 7-amino-actinomycin followed immediately by flow cytometric analysis. Ten thousand events of each sample were acquired on a Beckman Coulter FC500 Flow Cytometer.

Sulforhodamine B. The sulforhodamine B (SRB) assay was used according to the method of Skehan and colleagues (22). Cells were plated in 96-well flat-bottomed plates. After 24 hours, culture medium was replaced with fresh medium (with or without respective drugs) in triplicate or quadruplicate cultures. At the end of drug exposure (72 hours), cells were fixed for 1 hour and stained with 0.4% SRB (Sigma Aldrich), and the optical density was detected at 560 nm. Each experiment was repeated 3 times and figures depict a representative result. The specific DOG1 inhibitor A01 was kindly provided by Prof. Alan Verkman (University of California, San Francisco, CA).

Whole-cell patch-clamp. Whole-cell membrane currents were recorded in GIST-T1 and GIST882 cell lines. The extracellular (bath) solution had the following composition: 150 mmol/L NaCl, 1 mmol/L CaCl2, 1 mmol/L MgCl2, 10 mmol/L glucose, 10 mmol/L mannitol, 10 mmol/L Na-HEPES (pH = 7.4). The pipette (intracellular) solution contained 130 mmol/L CsCl, 10 mmol/L EGTA, 1 mmol/L MgCl2, 10 mmol/L HEPES, 1 mmol/L ATP (pH 7.4) plus CaCl2 to obtain the desired free $Ca2^+$ concentration: 8 mmol/L for 305 nmol/L (calculated with Patcher's Power Tool developed by Dr. Francisco Mendes and Franz Wurriehausen, Max Planck Institute for Biophysical Chemistry, Gottingen, Germany).

During experiments, the membrane capacitance and series resistance were analogically compensated using the circuitry provided by the EPC7 patch-clamp amplifier. The usual protocol for stimulation consisted of 600 ms long voltage steps from −100 to 100 mV in 20 mV increments starting from a holding potential of −60 mV. The waiting time between steps was 4 seconds. Membrane currents were filtered at 1 kHz and digitized at 5 kHz with an ITC-16 (Instrutech) AD/DA converter. Data were analyzed using the Igor software (Wavemetrics) supplemented by custom software kindly provided by Dr. Oscar Moran (Istituto di biofisica, Genova, Italy).

Western blotting. Whole-cell protein lysates were prepared from cell line monolayers according to standard protocols (23). Protein concentrations were determined with the Bio-Rad Protein Assay (Bio-Rad Laboratories). Proteins were separated by SDS/PAGE as described by Laemmli and colleagues (24) and transferred to Hybond-P membranes (Amersham Pharmacia Biotech). Changes in protein expression and phosphorylation as visualized by chemiluminescence (ECL chemi-luminescent reagent, Amersham Pharmacia Biotech) were captured and quantified using a FUJI LAS3000 system with Science Lab 2001 ImageGauge 4.0 software (Fujifilm Medial Systems).

In vivo studies

Tumor growth *in vivo* was evaluated by subcutaneously injecting the rear flanks of 6- to 8-week-old female adult athymic nude mice (NMRI nu/nu) with 10 million cells per flank transfected with scrambled or DOG1 shRNA. Tumor growth was monitored biweekly with a caliper, and tumor volumes were calculated by [(length × width^2)/2]. The experiment was stopped, mice were sacrificed, and tumors were harvested when controls reached approximately 1 cm^3. Statistical analysis of the mean tumor volumes was done by pairwise comparison using one-tailed homoscedastic *t* test analysis.

Immunhistochemical staining

Four micrometer sections of paraffin-embedded tissues of xenograft samples were cut and mounted onto SuperFrost Plus coated slides (Langenbrinck) for immunohistochemical staining. Heat-induced antigen retrieval (waterbath) was carried out with Target Retrieval Solution Citrate buffer (Dako) at pH 6.0 or HIER T-EDTA buffer (Zytomed Systems) at pH 9.0. Specimens were stained with a monoclonal rabbit anti-DOG1

Published OnlineFirst April 10, 2013; DOI: 10.1158/0008-5472.CAN-12-3839

[immunoglobulin G (IgG); clone, SP31; dilution, 1:100; 20 minutes, pH 6.0, Zytomed Systems, No. 504–3315], a monoclonal anti-Ki-67 (IgG1; clone, K-2; dilution, 1:2000; 30 minutes, pH 6.0, Zytomed Systems, No. MSK018), and a polyclonal anti-KIT antibody (dilution 1:200; 20 minutes, pH 9.0, Zytomed Systems, No. RP063) together with a highly sensitive and specific polymer detection system using horseradish peroxidase (ZytoChem-Plus HRP Polymer Kit, Zytomed Systems). The process for development was conducted using a permanent brown chromogenic substrate system (Permanent AEC Kit, Zytomed Systems). Finally, nuclei were counterstained with hematoxylin for 5 minutes.

RNA isolation and microarray gene expression profiling

Total RNA of cell line monolayers and tumor samples were isolated using the RNeasy Mini Kit (Qiagen), according to the manufacturer's instructions. Residual traces of genomic DNA were removed with DNase I (Qiagen). RNA concentration and purity were determined photometrically (NanoDrop, Thermo scientific). Preparation of cRNA targets (5 μg total RNA), fragmentation, hybridization of HG-U133 plus 2.0 microarrays (Affymetrix), washing, staining, and scanning were conducted according to manufacturer's protocols (Affymetrix) by the BioChip-Labor (Dr. Klein-Hitpass, Institute for Cell Biology, University of Duisburg-Essen, Essen, Germany). Signal intensities and detection calls were determined using Affymetrix microarray suite, version 5.0. Comparison files were further filtered to detect differentially expressed genes.

Quantitative real-time PCR

RNA extraction was conducted as described above, and cDNA synthesis was conducted using the RevertAid H Minus First Strand cDNA Synthesis Kit from Thermo Scientific. Quantitative real-time PCR (qRT-PCR) was carried out using TaqMan chemistry on the Roche LightCycler 480 (Roche) using the standard curve method in triplicate, as previously described (25). Probes for DOG1 (Hs00216121_m1), LTN1 (listerin E3 ubiquitin protein ligase 1, ID: Hs00391630_m1), MNK1 [mitogen-activated protein kinase (MAPK)-interacting serine/threonine kinase 1, ID: Hs00374376_m1), CDC14A (CDC14 cell division cycle 14 homolog A, ID: Hs00186432_m1), DDX17 [DEAD (Asp-Glu-Ala-Asp) box polypeptide 17, ID: Hs00428757_m1], insulin-like growth factor-binding protein 5 (IGFBP5, ID: Hs00181213_m1), EPHA4 (EPH receptor A4, ID: Hs00177874), and cyclin-dependent kinase inhibitor 1C (CDKN1C, ID: Hs00175938_m1) were purchased from Applied Biosystems (all FAM-labeled). Expression levels of the housekeeping gene *β-actin* (hs99999903_m1, FAM labeled) were assessed for normalization.

Whole transcriptome sequencing rRNA was depleted from 5 μg of total RNA using biotinylated oligonucleotides (Ribominus, Invitrogen), and libraries were constructed from the rRNA-depleted RNA according to the SOLiD Total RNA-seq Kit Protocol (Applied Biosystems). Briefly, library construction involved fragmentation of the RNA by RNAse III to an average size of 150 bases, ligation of the fragmented RNA to adaptors in a directed orientation, then cDNA synthesis, and PCR amplification of the resulting library. Approximately, 50 bases were sequenced from one end of each fragment using either the SOLiD 3+ or SOLiD 4 instrument and reagents (Applied Biosystems). The resulting sequence data were mapped to the human reference genome, hg18, using Bioscope v1.2 (Applied Biosystems). Sequences that mapped to unique locations were quantified per transcriptional unit, defined as "reads per kilobase of transcript per megabase of total sequence."

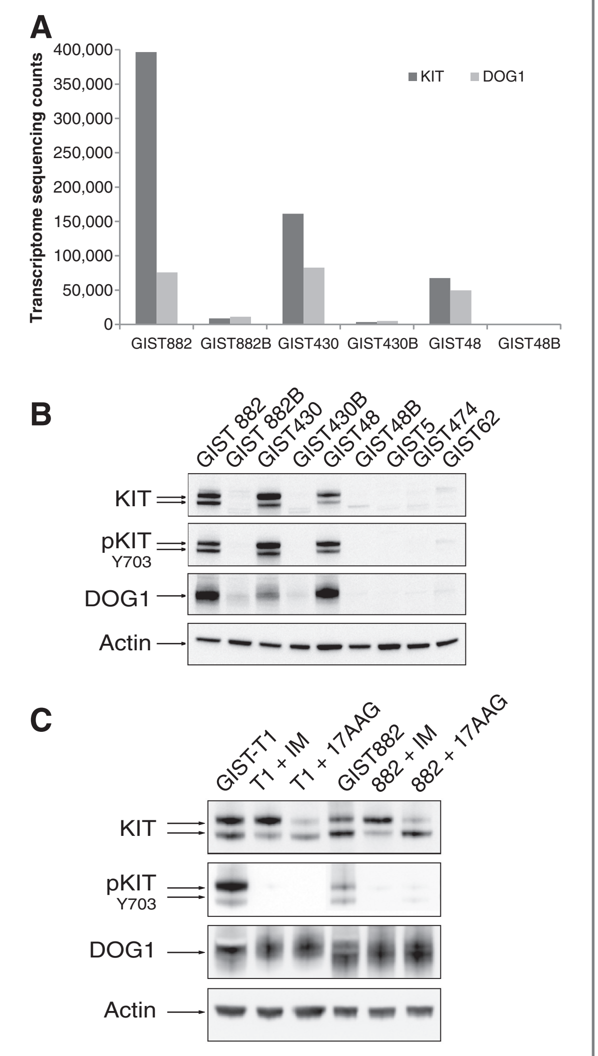

Figure 1. Coexpression of KIT and DOG1 in different GIST cell lines. A, whole transcriptome sequencing data for KIT and DOG1 in different GIST cell lines. B, Western blot analyses of KIT, pKIT, and DOG1 expression in KIT-positive (GIST882, GIST430, GIST48) and KIT-negative (GIST882B, GIST430B, GIST48B, GIST5, GIST474, GIST62) GIST cell lines. C, Western blot analyses of GIST-T1 and GIST882 after 24 hours of incubation with imatinib (1 μmol/l) and 17-AAG (500 nmol/L).

A weighted score, described by the following expression:

$$S_k = \frac{Y_k - X_k}{\sqrt{\max\,(X_k Y_k,\ 1000)}} \times log_{10}[\max(X_k Y_K,\ 1000)]$$

was used to rank the difference in reads for each transcript between samples.

Published OnlineFirst April 10, 2013; DOI: 10.1158/0008-5472.CAN-12-3839

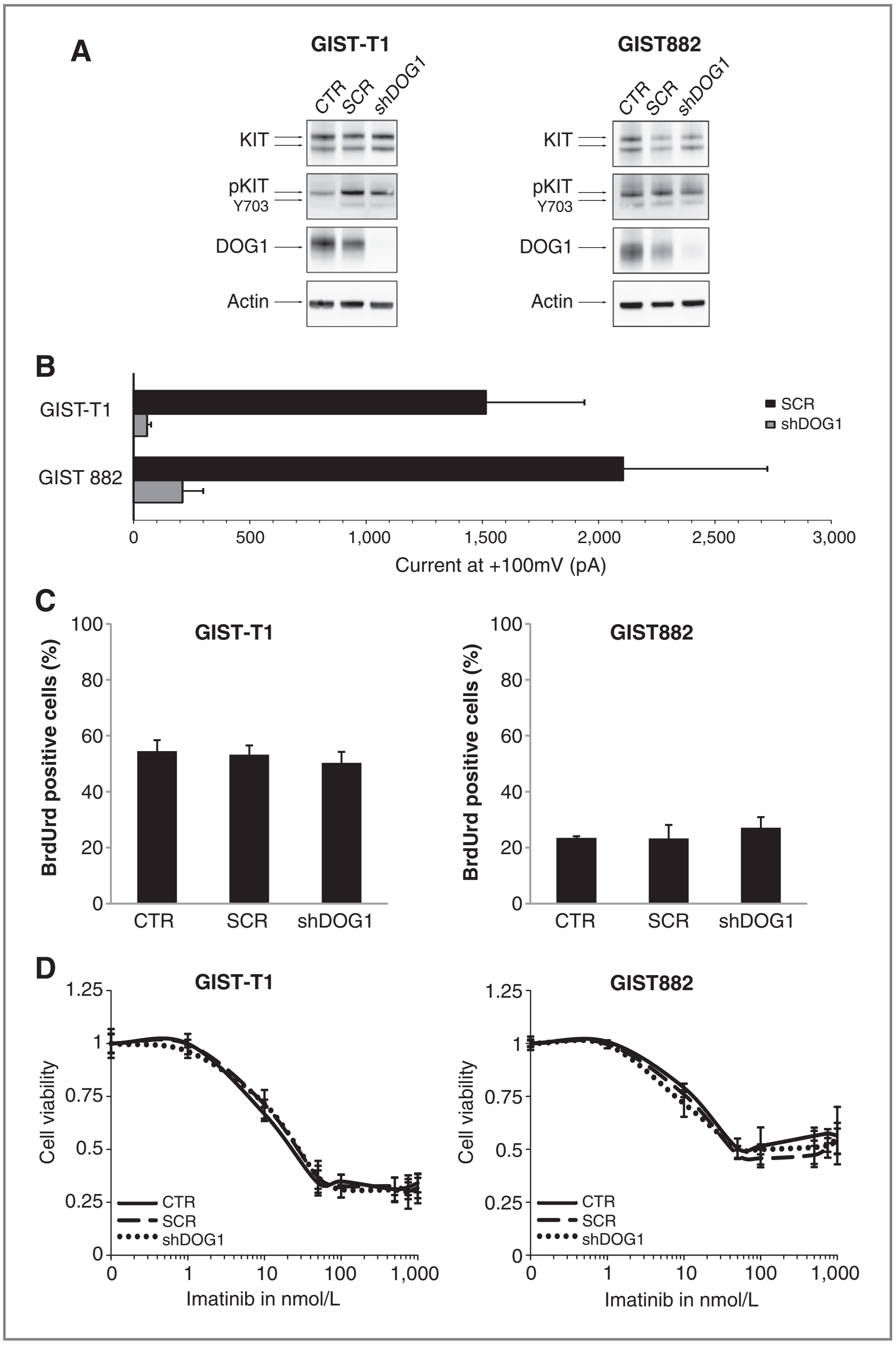

Figure 2. Effects of DOG1 knockdown. A, Western blot analyses of DOG1 expression in GIST-T1 and GIST882 cells. B, Whole-cell patch-clamp measurements of scrambled and DOG1 knockdown cells. C, BrdUrd cell proliferation assay. D, cells were treated for 72 hours with increasing doses of IM (1nm–10 μmol/L) and cytotoxicity was measured using SRB assays. Results represent the mean ± SD of quadruplicate values of a representative experiment.

Results

KIT and DOG1 are coexpressed in KIT-positive versus KIT-negative GIST cell lines

Whole transcriptome sequencing analyses of KIT-positive parental KIT cell lines and KIT-negative sublines showed a 47- to 157-fold reduction of KIT and a 7- to 77-fold reduction of DOG1 sequencing counts, suggestive of a coregulation (Fig. 1A). Immunoblot studies confirm this observation with an 83- to 99-fold reduction of DOG1 protein levels in KIT-negative GISTs (Fig. 1B). Direct (IM) or indirect (17-AAG) pharmacologic inhibition of KIT did not abolish DOG1 expression (Fig. 1C).

DOG1 knockdown does not affect KIT expression, cell proliferation, or IM sensitivity of GIST cells *in vitro*

To investigate the biologic role of DOG1 in GIST, GIST-T1 and GIST882 cells were transduced with lentiviral particles

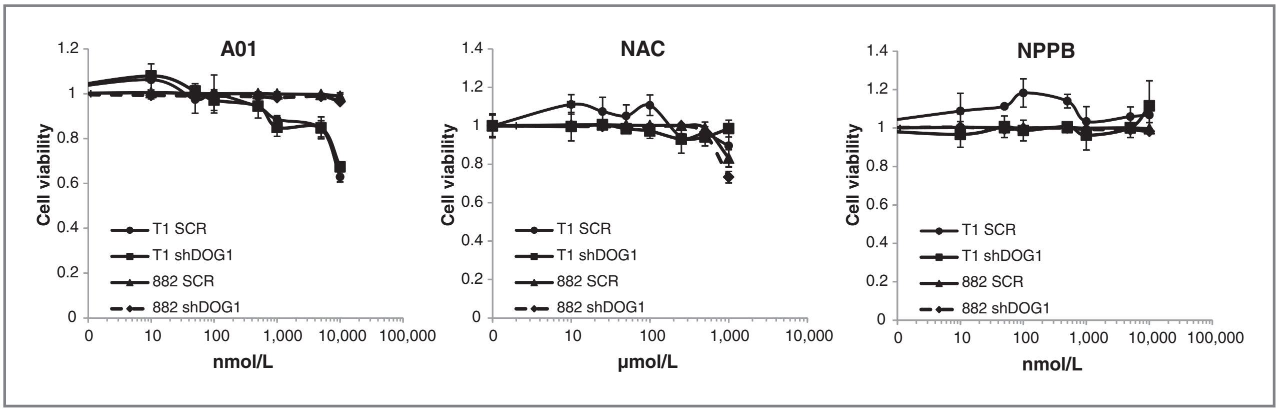

Figure 3. Cytotoxicity studies with the CaCC inhibitors A01, NAC, and NPPB. GIST-T1 and GIST882 cells with or without DOG1 knockdown were treated with increasing doses of inhibitors for 72 hours and the relative amount of remaining cells was measured using the SRB assay. Results represent the mean ± SD of quadruplicate values of a representative experiment.

carrying shRNAs against DOG1 (sequence: CCGGCGTC-GAGTTCAACGACAGAAACTCGAGTTTCTGTCGTTGAACTC-GACG TTTTTG). This resulted in a 91% reduction of DOG1 protein levels, whereas nonsense shRNA (scrambled) treatment did not alter DOG1 expression. Expression and activation of KIT and KIT-dependent signaling pathways were not altered by DOG1 knockdown (Fig. 2A).

Whole-cell patch-clamp experiments were carried out to confirm the functional effect of DOG1 reduction on chloride currents. Notably, DOG1 knockdown resulted in a 96% inhibition of chloride efflux in GIST-T1 and 90% in GIST882 compared with the controls, underscoring that DOG1 is a crucial regulator of GIST cell chlorine balance (Fig. 2B).

To assess the impact of DOG1 knockdown on cell proliferation, we conducted BrdUrd incorporation assays. Suppression of DOG1 did not significantly alter the proliferation of GIST-T1 and GIST882 cells *in vitro* (Fig. 2C). Moreover, IM sensitivity was maintained in both cell lines despite DOG1 knockdown, with IC_{50} values of 20 nmol/L and 50 nmol/L for GIST-T1 and GIST882 (Fig. 2D).

Biochemical inhibitors of CaCCs do not affect GIST cell growth *in vitro*

To further explore the functional impact of the DOG1 CaCC on GIST survival, GIST-T1 and GIST882 cells were treated for 3 days with 3 biochemical inhibitors of CaCCs, niflumic acid (NAC), 5-nitro-2-(3-phenylpropylamino)benzoic acid (NPPB), and A01 (being most specific for DOG1). At active concentrations (26), none of these CaCC inhibitors significantly reduced cell viability. The inhibition of GIST-T1 by A01 at 10 μmol/L (34%) was seen in both DOG1 knockdown and control cells and is therefore not a DOG1-specific effect (Fig. 3). Taken together, these findings argue against a cell-autonomous activity of DOG1 in GIST biology.

DOG1 knockdown inhibits growth of GIST xenografts in nude mice

As DOG1 might be involved tumor–host interactions in GIST, we next investigated the effect of DOG1 knockdown on tumor growth of GIST-T1, GIST882, and GIST430 *in vivo*. As shown in Fig. 4, DOG1 knockdown effectively suppressed DOG1 in all xenograft models (exemplified for GIST-T1 and GIST882), whereas xenografts from parental cells (no lentiviral transduction) and control cells (expressing scrambled shRNA) retained DOG1 expression as measured by immunoblot analysis (Fig. 4A) and immunohistochemistry (Fig. 4B). Interestingly, GIST-T1 tumors with DOG1 knockdown had lower proliferative activity (Ki-67: 60% positive cells in knockdown tumors vs. 90% in control tumors) resulting in a significant reduction (mean 43%) of tumor size after 19 days ($n = 8$; $P = 0.003$) compared with controls (Fig. 4C). A substantial growth delay (mean 31%) was also observed in GIST430, which exhibits an intrinsically slower tumor growth compared with GIST-T1. Notably, DOG1 knockdown did not alter the growth of GIST882 xenografts.

Analysis of gene expression data suggests IGFBP5 regulation by DOG1

To better understand the molecular consequences of DOG1 knockdown, we conducted expression arrays using Affymetrix HG-U133 plus 2.0 arrays containing 54,675 probe sets representing more than 24,568 human genes. Changes in expression were found in more than 1,500 genes after DOG1 knockdown in cell lines and in more than 3,500 genes after DOG1 knockdown in xenografts when compared with controls. As expected, *DOG1* (*ANO1*) was among the top-ranking differentially expressed genes. Other genes with strong differential expression are shown in Fig. 5 and Supplementary Tables S1 and S2. Comprehensive pathway analyses were conducted using Ingenuity Pathway Analysis (Ingenuity Systems). For those, a fold-change cutoff was set at ≥1 to identify genes whose expression was significantly differentially up- or downregulated.

Comparison of microarray data with qRT-PCR data

We conducted a literature search on the 40 top-ranking, differentially expressed genes. Genes that might have an impact on proliferation or apoptosis were selected for qRT-PCR validation. Among these candidates, a substantial (> 3-

Published OnlineFirst April 10, 2013; DOI: 10.1158/0008-5472.CAN-12-3839

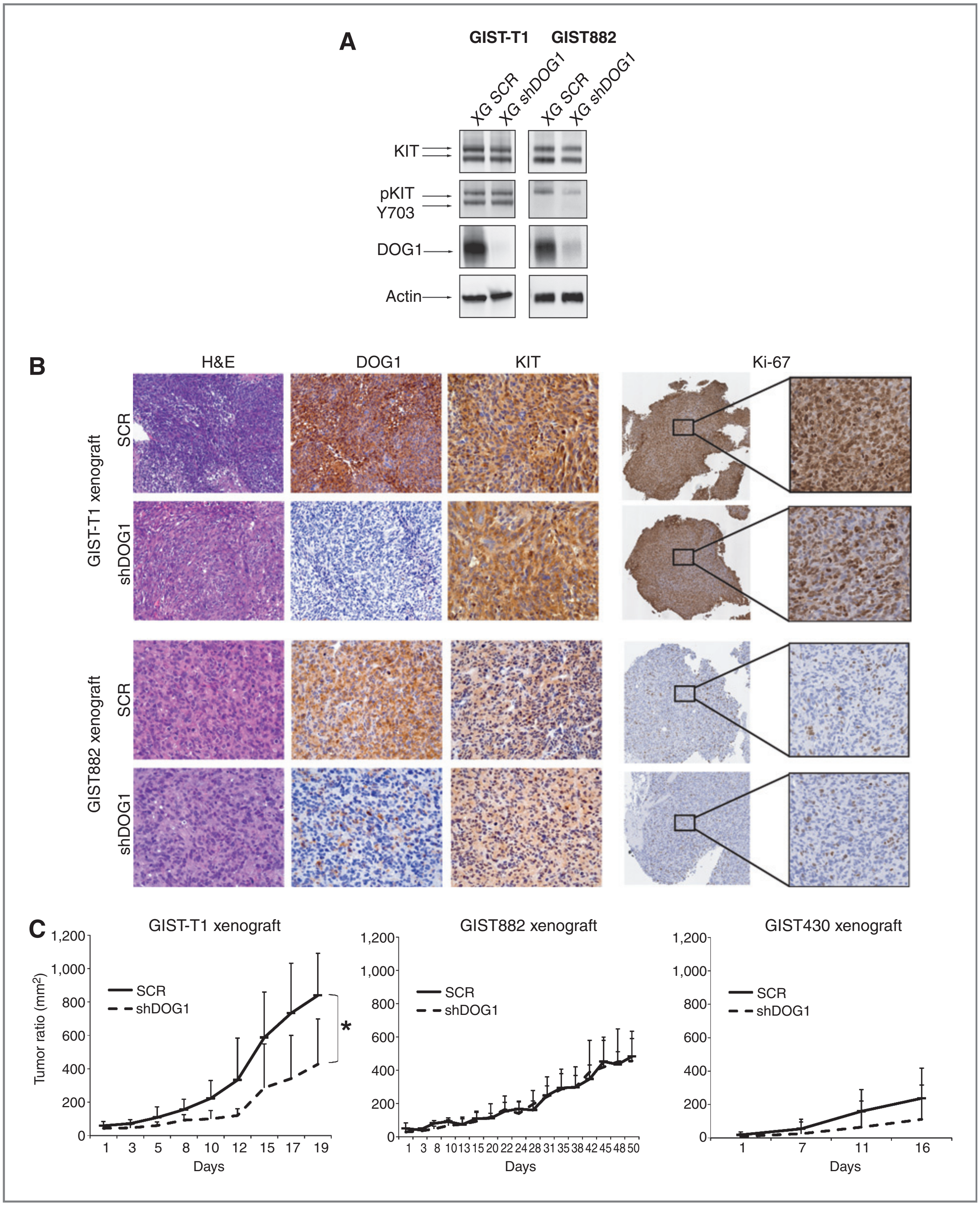

Figure 4. *In vivo* growth of DOG1 knockdown xenografts. A, Western blot analyses of DOG1 and KIT expression in GIST-T1 and GIST882 xenografts. B, immunohistochemical analysis of GIST-T1 and GIST882 xenografts. Samples were stained with hematoxylin and eosin (H&E) and with antibodies against DOG1, KIT, and Ki-67. C, tumor volume over time in nude mice implanted with GIST-T1, GIST882, and GIST430 cells after shRNA-mediated DOG1 suppression compared with scrambled shRNA controls. *, $P = 0.003$.

Published OnlineFirst April 10, 2013; DOI: 10.1158/0008-5472.CAN-12-3839

Figure 5. Heat map representing color-coded expression levels of differentially expressed genes [upregulated (red) or downregulated (green)] in GIST-T1 xenograft and cell line.

fold) difference in expression levels was found for *DOG1* and *IGFBP5*, whereas levels of other candidates were only marginally changed (Fig. 6A). IGFBP5 levels decreased in GIST882 upon DOG1 knockdown (Fig. 6B). In DOG1-negative GIST882B, *IGFBP5* transcript counts were unchanged compared with the parental DOG1-positive GIST882 cell line. Notably, DOG1-negative GIST430B cell line showed *IGFBP5* transcriptome sequencing counts that were 5,000-fold higher than that in the parental DOG1-positive GIST430 cell line (Fig. 6C). The Ingenuity Pathway Analysis suggested the IGF pathway together with paxillin signaling as the top-ranking pathways affected by the DOG1 knockdown.

Discussion

With the introduction of imatinib, a potent KIT inhibitor, the treatment of GIST as a mainly KIT/PDGFRA-driven sarcoma has been revolutionized. Most patients whose tumors harbor activating KIT mutations benefit from IM-treatment with a median progression-free survival of 12 to 24 months (27). Although a subset of patients remains free of progression, the majority eventually progress, at which point their therapeutic options are limited. Novel treatment strategies to prevent or overcome resistance are therefore urgently needed.

DOG1 (Ano1/TMEM16A), a CaCC, was identified in microarray studies among a number of genes whose expression was significantly higher in GIST than in other soft tissue sarcomas (13, 28). It has since then proven to be a reliable immunohistochemical marker in pathologic practice (17). Mutations of *DOG1* have not been found in GIST (29) but expression levels are also high in ICC, the cells thought to share a common progenitor with GIST (14, 15). Whether DOG1 is a lineage-specific marker that plays a role in differentiation or also might play a transforming role in GIST is yet unclear.

To our knowledge, we are the first to investigate DOG1 biologic roles and to assess DOG1 relevance as therapeutic target in GIST.

Pathologic and genetic analyses from resected metastases progressing on imatinib have revealed secondary KIT mutations as a common mechanism of resistance. In a subset of patients, GIST metastases have lost KIT expression, indicating that KIT oncogenic programs have been supplanted by yet unidentified alternative oncogenic drivers (30). We observed a similar phenomenon in sublines of several GIST cell lines, which lost KIT expression during cultivation *ex vivo*. Interestingly, these cell lines also lost DOG1 expression suggesting interdependence of expression. Notably, the majority of KIT-negative GIST tumors (64%) in clinical practice also do not express DOG1 (17).

In the studies reported herein, DOG1 knockdown resulted in strong functional inhibition of chloride currents but did not affect expression or activation of KIT and KIT-dependent signaling pathways (Fig. 2A; data not shown). In our models, DOG1 therefore does not act as key regulator of KIT, and our studies suggest that DOG1 inhibition will not synergize with KIT kinase–inhibitor drugs in inactivating KIT. Whether DOG1 expression is directly coregulated with KIT is yet unknown; however, biochemical inhibition of KIT does not affect DOG1 expression (Fig. 1C) *in vitro*. We further showed that neither DOG1 knockdown nor biochemical inhibitors of DOG1 alter the growth modulating effect of imatinib *in vitro*. However, we observed a substantial growth delay when GIST-T1 and GIST430 were grown as xenografts compared with scrambled controls in nude mice. This effect was not seen in GIST882.

DOG1 is expressed in many organs (e.g., salivary glands) and DOG1 knockout mice die soon after birth (10, 31, 32). Little is known about DOG1 expression in human tissues but the UniGene database suggests an expression pattern similar to that in mice (33). Nonetheless, DOG1 expression is still remarkably high in both GIST and ICCs compared with non-GIST sarcomas (13, 16). Notably, Stanich and colleagues showed growth inhibitory effects after DOG1 knockdown and DOG1

Published OnlineFirst April 10, 2013; DOI: 10.1158/0008-5472.CAN-12-3839

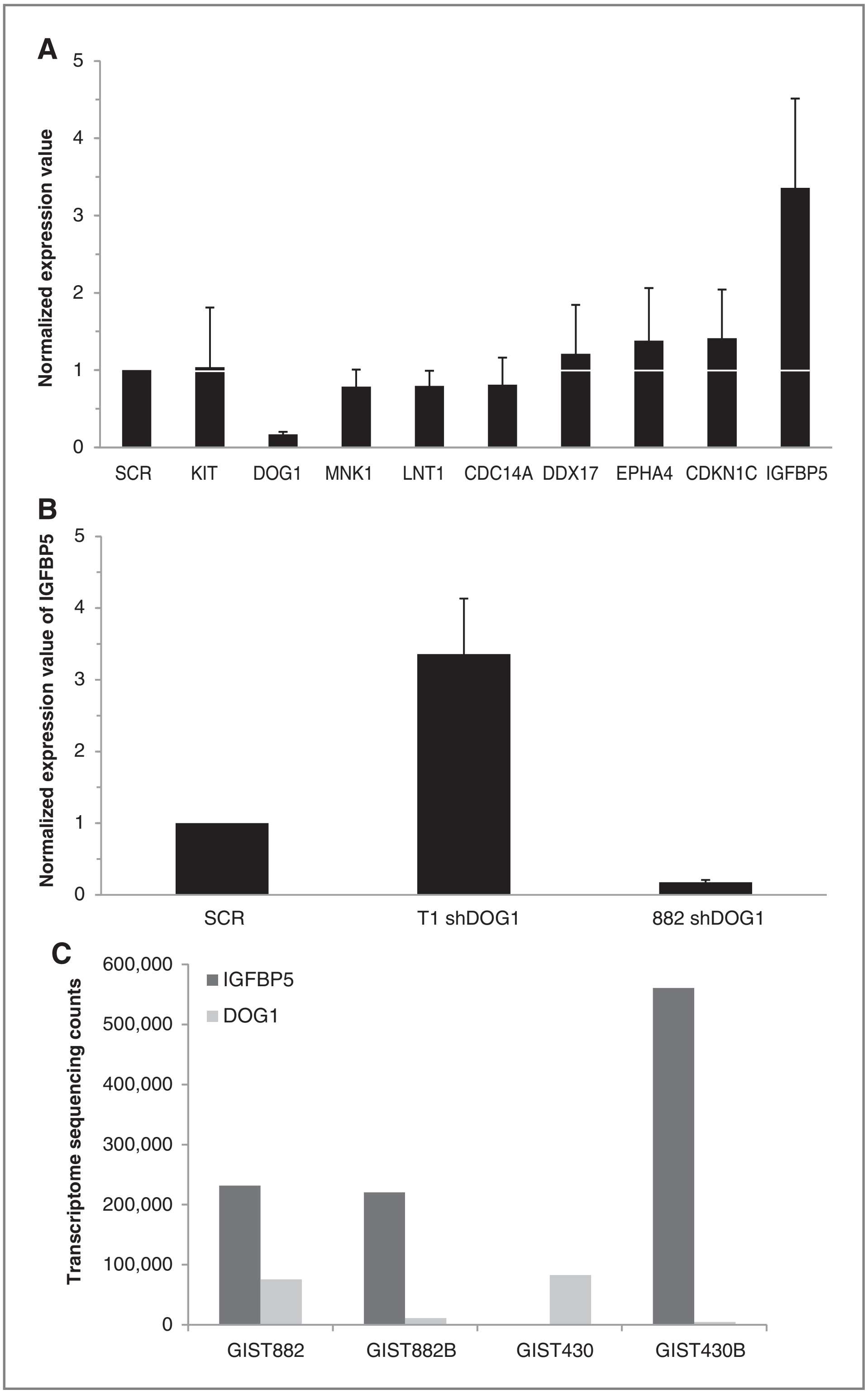

Figure 6. Analysis of gene expression data. A, quantitative real-time RT-PCR evaluation of KIT, DOG1, MNK1 (MAPK interacting serine/threonine kinase 1), LTN1 (listerin E3 ubiquitin protein ligase 1), CDC14A (CDC14 cell division cycle 14 homolog A), DDX17 [DEAD (Asp-Glu-Ala-Asp) box polypeptide 17], EPHA4 (EPH receptor A4), CDKN1C, and IGFBP5 mRNA in GIST-T1 xenografts. B, quantitative real-time RT-PCR evaluation of IGFBP5 in GIST-T1 and GIST882. Values were normalized to the scrambled control. C, whole transcriptome sequencing data for IGFBP5 in GIST882 (KIT- and DOG1-positive), GIST882B (KIT- and DOG1-negative), GIST430 (KIT- and DOG1-positive), and GIST430B (KIT- and DOG1-negative) cells.

biochemical inhibition in ICC short-term cultures (34). They concluded that regulation of proliferation by DOG1 is related to its function as a Cl^- entry pathway by reducing the Cl^- concentration in the culture media. In contrast to Stanich and colleagues, we did not observe a reduction of phosphorylated retinoblastoma tumor suppressor protein (Rb; data not shown), as a possible explanation for a cell-cycle arrest (35).

DOG1 has also been linked to other types of cancers. Amplification of the chromosomal band 11q13, the genomic

Published OnlineFirst April 10, 2013; DOI: 10.1158/0008-5472.CAN-12-3839

region containing DOG1, is frequently seen in breast, bladder, head and neck, and esophageal cancer (36). Patients with squamous cell carcinomas of the head and neck (SCCHN) harboring 11q13 amplifications were associated with a poor prognosis. These findings were recently confirmed by functional studies in SCCHN cell lines that showed that DOG1 amplification was associated with increased spreading, detachment, and invasion of tumor cells (37). Similar to our findings, Duvvuri and colleagues observed inhibition of tumor growth in SCCHN xenografts after knockdown of DOG1 (38). Notably, this effect was also seen *in vitro*.

We did not find published evidence that provides simple answers as to why a DOG1 knockdown would affect cell growth *in vivo* but not *in vitro*, as seen in our models. We speculate that the more complex cell–cell interaction in 3-dimensional tumors compared with monolayers as well as a tumor/hostinteraction (e.g., vasculature) may be responsible for this effect.

Using gene expression analyses, we investigated differentially expressed genes that are directly associated with proliferation or survival. Pathway analyses using Ingenuity software suggested IGF- and paxillin signaling as the most relevant pathways affected by DOG1 knockdown. Although the change of expression levels of genes involved in the paxillin pathway was subtle, IGFBP5 was the strongest differentially expressed gene besides DOG1 as confirmed by qRT-PCR. In line with these findings, the GIST cell line GIST430B, a KIT-negative, and DOG1-negative subline of imatinib-resistant GIST430, showed a 5,000-fold increase of IGFBP5 transcripts compared with its parental DOG1-positive GIST430 cell line. IGFBP5 was not upregulated in GIST882 following DOG1 knockdown, and no growth delay was observed *in vivo* suggesting that IGFBP5 may not be relevant to all GIST.

IGFBP5 is one of the 6 IGFBP family members and is dysregulated in diverse types of cancer including breast cancer (39), ovarian cancer (40), and Rb (41). IGFBP5 overexpression results in "trapping" of IGF1 and IGF2 with subsequent inhibition of the IGF axis pathway (42). Of note, IGFBP5 has recently been shown to suppress tumor growth and metastasis of human osteosarcomas (43). In another model, IGFBP5 overexpression prevented tumor growth by inhibition of tumor vascularity, which might explain the different biologic outcomes we found between our *in vivo* and *in vitro* experiments. Interestingly, IGF2 expression has recently been shown to predict a high mitotic index correlating with outcome in GIST underlining the relevance of the IGF axis in GIST (44). DOG1 expression was also reported to promote tumor growth through activation of the (MAPK) pathway (38), which we did not observe in our models (data not shown). Of note, MAPK activation in imatinib-sensitive GIST models is usually strongly dependent on KIT activation (45).

Given its high levels of expression, DOG1 could represent a tumor-specific target in GIST. Tumor growth in our models was not dependent on DOG1 *in vitro* and only partially dependent *in vivo*. These findings suggest a potential therapeutic role only in combination with other drugs. In addition, further efforts are needed to identify biochemical inhibitors with improved selectivity for DOG1, which recapitulate the effects seen upon DOG1 knockdown *in vivo*. At present, clinical evaluation of DOG1 inhibitors may be constrained by their concomitant inhibition of other chloride channels.

Our results highlight the functional relevance of DOG1 in a subset of GIST and suggest that further studies are warranted to better understand DOG1 and IGF1 axis growth regulation roles in GIST.

Disclosure of Potential Conflicts of Interest

M. Schuler has commercial research grant, has honoraria from speakers' bureau, and is a consultant/advisory board member of Novartis. S. Bauer has honoraria from speakers' bureau from GIST. No potential conflicts of interest were disclosed by the other authors.

Authors' Contributions

Conception and design: S. Simon, T. Muehlenberg, G. Taeger, S. Bauer
Development of methodology: S. Simon, T. Muehlenberg, S. Bauer
Acquisition of data (provided animals, acquired and managed patients, provided facilities, etc.): S. Simon, L.J.V. Galietta, B. Schwindenhammer, G. Taeger, G. Eilers, M. Schuler, J.A. Fletcher, S. Bauer
Analysis and interpretation of data (e.g., statistical analysis, biostatistics, computational analysis): S. Simon, F. Grabellus, L. Ferrera, L.J.V. Galietta, T. Muehlenberg, F. Breitenbuecher, M. Schuler, J.A. Fletcher, S. Bauer
Writing, review, and/or revision of the manuscript: S. Simon, F. Grabellus, L. Ferrera, T. Muehlenberg, J. Treckmann, F. Breitenbuecher, M. Schuler, J.A. Fletcher, S. Bauer
Administrative, technical, or material support (i.e., reporting or organizing data, constructing databases): G. Taeger, M. Schuler, T. Taguchi, S. Bauer
Study supervision: S. Bauer

Acknowledgments

The authors sincerely thank the expert technical assistance received from Miriam Backs and Julia Ketzer.

Grant Support

This work was supported by funding from Max-Eder Fellowship from the Deutsche Krebshilfe (S. Bauer), the Life Raft Group Research Initiative (S. Bauer and J.A. Fletcher), and NIH GI SPORE 1P50CA12703-05. The funders had no role in study design, data collection and analysis, decision to publish, or preparation of the manuscript.

The costs of publication of this article were defrayed in part by the payment of page charges. This article must therefore be hereby marked *advertisement* in accordance with 18 U.S.C. Section 1734 solely to indicate this fact.

Received October 4, 2012; revised February 15, 2013; accepted March 20, 2013; published OnlineFirst April 10, 2013.

References

1. Heinrich MC, Corless CL, Duensing A, McGreevey L, Chen C-J, Joseph N, et al. PDGFRA activating mutations in gastrointestinal stromal tumors. Science 2003;299:708–10.
2. Hirota S. Gain-of-function mutations of c-kit in human gastrointestinal stromal tumors. Science 1998;279:577–80.
3. Rubin BP, Singer S, Tsao C, Duensing A, Lux ML, Ruiz R, et al. KIT activation is a ubiquitous feature of gastrointestinal stromal tumors. Cancer Res 2001;61:8118–21.
4. Blanke CD, Demetri GD, Von Mehren M, Heinrich MC, Eisenberg B, Fletcher JA, et al. Long-term results from a randomized phase II trial of standard- versus higher-dose imatinib mesylate for patients with unresectable or metastatic gastrointestinal stromal tumors expressing KIT. J Clin Oncol 2008;26:620–5.
5. Demetri G, von Mehren M, Blanke CD, Abbeele van den AD, Eisenberg BL, Roberts PJ, et al. Efficacy and safety of imatinib mesylate in advanced gastrointestinal stromal tumors. N Engl J Med 2002;347:472–80.

Published OnlineFirst April 10, 2013; DOI: 10.1158/0008-5472.CAN-12-3839

6. Wardelmann E, Thomas N, Merkelbach-bruse S, Pauls K, Speidel N, Büttner R, et al. Acquired resistance to imatinib in gastrointestinal stromal tumours caused by multiple KIT mutations. Lancet Oncol 2005;6:249–51.
7. Heinrich MC, Corless CL, Blanke CD, Demetri GD, Joensuu H, Roberts PJ, et al. Molecular correlates of imatinib resistance in gastrointestinal stromal tumors. J Clin Oncol 2006;24:4764–74.
8. Caputo A, Caci E, Ferrera L, Pedemonte N, Barsanti C, Sondo E, et al. TMEM16A, a membrane protein associated with calcium-dependent chloride channel activity. Science 2008;322:590–4.
9. Schroeder BC, Cheng T, Jan YN, Jan LY. Expression cloning of TMEM16A as a calcium-activated chloride channel subunit. Cell 2008;134:1019–29.
10. Yang YD, Cho H, Koo JY, Tak MH, Cho Y, Shim W-S, et al. TMEM16A confers receptor-activated calcium-dependent chloride conductance. Nature 2008;455:1210–5.
11. Huang F, Rock JR, Harfe BD, Cheng T, Huang X, Jan YN, et al. Studies on expression and function of the TMEM16A calcium-activated chloride channel. Proc Natl Acad Sci U S A 2009;106:21413–8.
12. Hwang SJ, Blair PJA, Britton FC, Hennig G, Bayguinov YR, Rock JR, et al. Expression of anoctamin 1/TMEM16A by interstitial cells of Cajal is fundamental for slow wave activity in gastrointestinal muscles. J Physiol 2009;587:4887–904.
13. West RB, Corless CL, Chen X, Rubin BP, Subramanian S, Montgomery K, et al. The novel marker, DOG1, is expressed ubiquitously in gastrointestinal stromal tumors irrespective of KIT or PDGFRA mutation status. Am J Pathol 2004;165:107–13.
14. Chen H, Ordog T, Chen J, Young DL, Bardsley MR, Redelman D, et al. Differential gene expression in functional classes of interstitial cells of Cajal in murine small intestine. Physiol Genomics 2007;31:492–509.
15. Gomez-Pinilla PJ, Gibbons SJ, Bardsley MR, Lorincz A, Pozo MJ, Pasricha PJ, et al. Ano1 is a selective marker of interstitial cells of Cajal in the human and mouse gastrointestinal tract. Am J Physiol Gastrointest Liver Physiol 2009;296:G1370–81.
16. Espinosa I, Lee C-H, Kim MK, Rouse B-T, Subramanian S, Montgomery K, et al. A novel monoclonal antibody against DOG1 is a sensitive and specific marker for gastrointestinal stromal tumors. Am J Surg Pathol 2008;32:210–8.
17. Liegl B, Hornick JL, Corless CL, Fletcher CDM. Monoclonal antibody DOG1.1 shows higher sensitivity than KIT in the diagnosis of gastrointestinal stromal tumors, including unusual subtypes. Am J Surg Pathol 2009;33:437–46.
18. Miettinen M, Wang Z-F, Lasota J. DOG1 antibody in the differential diagnosis of gastrointestinal stromal tumors: a study of 1840 cases. Am J Surg Pathol 2009;33:1401–8.
19. Taguchi T, Sonobe H, Toyonaga S-ichi, Yamasaki I, Shuin T, Takano A, et al. Conventional and molecular cytogenetic characterization of a new human cell line, GIST-T1, established from gastrointestinal stromal tumor. Lab Invest 2002;82:663.
20. Tuveson DA, Willis NA, Jacks T, Griffin JD, Singer S, Fletcher CDM, et al. STI571 inactivation of the gastrointestinal stromal tumor c-KIT oncoprotein: biological and clinical implications. Oncogene 2001;20:5054–8.
21. Bauer S, Yu LK, Demetri GD, Fletcher JA. Heat shock protein 90 inhibition in imatinib-resistant gastrointestinal stromal tumor. Cancer Res 2006;66:9153–61.
22. Skehan P, Storeng R, Scudiero D, Monks A, McMahon J, Vistica D, et al. New colorimetric cytotoxicity assay for anticancer-drug screening. J Natl Cancer Inst 1990;82:1107–12.
23. Duensing A, Medeiros F, McConarty B, Joseph NE, Panigrahy D, Singer S, et al. Mechanisms of oncogenic KIT signal transduction in primary gastrointestinal stromal tumors (GISTs). Oncogene 2004;23:3999–4006.
24. Laemmli UK. Cleavage of structural proteins during the assembly of the head of bacteriophage T4. Nature 1970;227:680–5.
25. Bustin SA. Absolute quantification of mRNA using real-time reverse transcription polymerase chain reaction assays. J Mol Endocrinol 2000;25:169–93.
26. Namkung W, Phuan P-W, Verkman AS. TMEM16A inhibitors reveal TMEM16A as a minor component of calcium-activated chloride channel conductance in airway and intestinal epithelial cells. J Biol Chem 2011;286:2365–74.
27. Heinrich MC, Owzar K, Corless CL, Hollis D, Borden EC, Fletcher CDM, et al. Correlation of kinase genotype and clinical outcome in the North American Intergroup Phase III Trial of imatinib mesylate for treatment of advanced gastrointestinal stromal tumor: CALGB 1501;05 Study by Cancer and Leukemia Group B and Southwest Oncology Group. J Clin Oncol 2008;26:5360–7.
28. Allander SV, Nupponen NN, Ringnér M, Ringne M, Hostetter G, Maher GW, et al. Gastrointestinal stromal tumors with KIT mutations exhibit a remarkably homogeneous gene expression profile advances in brief gastrointestinal stromal tumors with KIT mutations exhibit a remarkably homogeneous gene expression profile 1. Cancer Res 2001;61:8624–8.
29. Miwa S, Nakajima T, Murai Y, Takano Y, Sugiyama T. Mutation assay of the novel gene DOG1 in gastrointestinal stromal tumors (GISTs). J Gastroenterol 2008;43:531–7.
30. Bauer S, Hartmann JT, de Wit M, Lang H, Grabellus F, Antoch G, et al. Resection of residual disease in patients with metastatic gastrointestinal stromal tumors responding to treatment with imatinib. Int J Cancer 2005;117:316–25.
31. Rock JR, Futtner CR, Harfe BD. The transmembrane protein TMEM16A is required for normal development of the murine trachea. Dev Biol 2008;321:141–9.
32. Schreiber R, Uliyakina I, Kongsuphol P, Warth R, Mirza M, Martins JR, et al. Expression and function of epithelial anoctamins. J Biol Chem 2010;285:7838–45.
33. Kunzelmann K, Kongsuphol P, Aldehni F, Tian Y, Ousingsawat J, Warth R, et al. Bestrophin and TMEM16-Ca(2+) activated Cl(-) channels with different functions. Cell Calcium 2009;46:233–41.
34. Stanich JE, Gibbons SJ, Eisenman ST, Bardsley MR, Rock JR, Harfe BD, et al. Ano1 as a regulator of proliferation. Am J Physiol Gastrointest Liver Physiol 2011 301:1044–51.
35. Giacinti C, Giordano A. RB and cell cycle progression. Oncogene 2006;25:5220–7.
36. Akervall JA, Jin Y, Wennerberg JP, Zätterström UK, Kjellén E, Mertens F, et al. Chromosomal abnormalities involving 11q13 are associated with poor prognosis in patients with squamous cell carcinoma of the head and neck. Cancer 1995;76:853–9.
37. Ayoub C, Wasylyk C, Li Y, Thomas E, Marisa L, Robé A, et al. ANO1 amplification and expression in HNSCC with a high propensity for future distant metastasis and its functions in HNSCC cell lines. Br J Cancer 2010;103:715–26.
38. Duvvuri U, Shiwarski DJ, Xiao D, Bertrand C, Huang X, Edinger RS, et al. TMEM16A, induces MAPK and contributes directly to tumorigenesis and cancer progression. Cancer Res 2012;72;3270–81.
39. Ahn BY, Elwi AN, Lee B, Trinh DLN, Klimowicz AC, Yau A, et al. Genetic screen identifies insulin-like growth factor binding protein 5 as a modulator of tamoxifen resistance in breast cancer. Cancer Res 2010;70:3013–9.
40. Walker G, MacLeod K, Williams ARW, Cameron DA, Smyth JF, Langdon SP. Insulin-like growth factor binding proteins IGFBP3, IGFBP4, and IGFBP5 predict endocrine responsiveness in patients with ovarian cancer. Clin Cancer Res 2007;13:1438–44.
41. Xu XL, Lee TC, Offor N, Cheng C, Liu A, Fang Y, et al. Tumor-associated retinal astrocytes promote retinoblastoma cell proliferation through production of IGFBP-5. Am J Pathol 2010;177:424–35.
42. Beattie J, Allan GJ, Lochrie JD, Flint DJ. Insulin-like growth factor-binding protein-5 (IGFBP-5): a critical member of the IGF axis. Biochem J 2006;395:1–19.
43. Su Y, Wagner ER, Luo Q, Huang J, Chen L, He B-C, et al. Insulin-like growth factor binding protein 5 suppresses tumor growth and metastasis of human osteosarcoma. Oncogene 2011;30:3907–17.
44. Braconi C, Bracci R, Bearzi I, Bianchi F, Sabato S, Mandolesi A, et al. Insulin-like growth factor (IGF) 1 and 2 help to predict disease outcome in GIST patients. Ann Oncol 2008;19:1293–8.
45. Bauer S, Duensing A, Demetri GD, Fletcher JA. KIT oncogenic signaling mechanisms in imatinib-resistant gastrointestinal stromal tumor: PI3-kinase/AKT is a crucial survival pathway. Oncogene 2007;26:7560–8.

Published OnlineFirst April 10, 2013; DOI: 10.1158/0008-5472.CAN-12-3839

Cancer Research
The Journal of Cancer Research (1916–1930) | The American Journal of Cancer (1931–1940)

American Association for Cancer Research

DOG1 Regulates Growth and IGFBP5 in Gastrointestinal Stromal Tumors

Susanne Simon, Florian Grabellus, Loretta Ferrera, et al.

Cancer Res 2013;73:3661-3670. Published OnlineFirst April 10, 2013.